Supporting Information

Colorimetric and electrochemical integrated dual-mode detection for glucose by utilizing CoOOH@Cu nanosheets as peroxidase mimetics

Hong Cheng, Zhaoyang Wang, Huanhuan Sun, Biao Chen, Jin Huang, Ruichen Jia, Xiaoxiao He*, Kemin Wang*

State Key Laboratory of Chemo/Biosensing and Chemometrics, College of Biology, College of Chemistry and Chemical Engineering, Hunan University, Key Laboratory for Bio-Nanotechnology and Molecule Engineering of Hunan Province, Changsha 410082, China.

Experimental Section

Chemicals and Materials. *o*-phenylenediamine (OPD), $CuCl_2$, NaClO, uric acid (UA) and horseradish peroxidase (HRP) were purchased from Shanghai Sangon Biotech (Shanghai, China). KCl, NaAc, HAc, HCl, 30% H_2O_2, glucose, sucrose, lactose, *L*-cysteine, ascorbic acid (AA), dopamine and NaOH were purchased from Sinopharm Chemical Reagents (Shanghai, China). $CoCl_2 \cdot 6H_2O$ and glucose oxidase (GOx) were obtained from Sigma Aldrich Trading Co., LTD (Louis, U. S. A.). Sterilization of water was employed in all operation procedures (Milli Q system, 18.2 MΩ cm). All data of UV-vis spectrum was obtained from an Epoch-2 Microplate Reader (BioTeck Instruments, U. S. A.). The Fourier-transform infrared (FTIR) spectrum was obtained from the equipment of Bruker Tensor 27 (Karlsruhe, Germany). The X-ray photoelectron spectroscopy (XPS) spectrum was collected from an ESCALAB 250Xi (ThermoFisher Scientific, U. S. A.). All electrochemical measurements were operated on the Chenhua CHI660A electrochemical working station (Shanghai, China).

The NaAc buffer was consisted of 200 mM NaAc, 100 mM KCl, the pH value was distributed from 2.0 to 9.0, respectively.

The glucose and GOx buffer were both prepared from NaAc buffer by adjusting the pH to 5.5.

Synthesis of the CoOOH and CoOOH@Cu nanosheet. The CoOOH nanosheet was prepared as our reported procedure with few modifications. In brief, the mixture of 1 mL 100 mM NaOH solution and 2 mL 10 mM $CoCl_2$ solution was drawn repeatedly by pipettor under sonication for 120 seconds, soon another 0.2 mL of NaClO solution was dropped. Similarly, the mixture was drawn repeatedly by pipettor under sonication for 600 seconds. After centrifugation of purification, the CoOOH nanosheet was collected and dried in vacuum for further use.

The CoOOH@Cu nanosheet was prepared as similar method. The mixture of 1 mL 100 mM NaOH solution, 2 mL 10 mM $CoCl_2$ solution and 200 μL $CuCl_2$ solution with suitable concentration was drawn repeatedly by pipettor under sonication for 120 seconds, soon another 0.2 mL of NaClO solution was dropped. Similarly, the mixture was drawn repeatedly by pipettor under sonication for 600 seconds. After centrifugation of purification, the CoOOH@Cu nanosheet was collected and dried in vacuum for further use.

The peroxidase-like activity of CoOOH@Cu nanosheet. In a 10 mL centrifuge tube, 40 μL of 50 μg /mL CoOOH@Cu solution, 80 μL 15 mM OPD solution, 80 μL different concentration H_2O_2 solution was added to 7.8 mL 200 mM NaAc buffer (pH = 4.0). The mixed solution was incubated under 50 °C for about 20 min, the samples were taken for photograph under white-light and recorded with UV absorption and electrochemical signals.

The comparison of peroxidase-like activity of CoOOH and CoOOH@Cu nanosheet. The peroxidase-like activities of CoOOH and CoOOH@Cu nanosheet were compared by incubating with the mixed solution of 15 mM OPD and 10 mM H_2O_2 solutions in NaAc buffer (pH = 4.0). The UV absorbance spectra and DPV signals were recorded.

The kinetic Assay. The kinetic data was measured by adjusting the different concentrations of reaction substrate OPD or H_2O_2. The kinetic data was obtained following the Michaelis-Menten equation:

$$\mathbf{v} = \frac{\mathbf{Vmax} \cdot \mathbf{S}}{\mathbf{K_m} + \mathbf{S}}$$

where v stands for the primal velocity, Vmax means the maximal reaction velocity, S stands for the molar concentration of OPD or H_2O_2, and Km is corresponding to the Michaelis constant.

Glucose Detection. The monitoring of glucose levels was operated as the bellowing procedures: In a 10 mL centrifuge tube, a mixed solution containing 16 μL of 5 mg/mL GOx, 200 μL different concentrations of glucose were reacted at 37 °C for 30 min. Then, 40 μL of 50 μg /mL CoOOH@Cu solution, 80 μL 15 mM OPD solution, 7.8 mL 200 mM NaAc buffer (pH = 4.0) were added into the centrifuge tube. After incubating at 50 °C for another 20 min, the samples were taken for photograph under white-light and recorded with UV absorption and electrochemical signals. In selective experiments, sucrose, lactose, *L*-cysteine, ascorbic acid (AA), uric acid (UA), and dopamine with the 10 times the concentration than glucose were selected as interferences, and the operation steps were close to glucose.

Real sample preparation.

The rat blood was collected from eyes and stored in blood collection tube (with EDTA-2Na), then centrifuged under 2000 rpm for 20 min. Then the serum was collected and diluted with sterile water to prepare 20%, 10% and 4% serum samples. All animal care and experimental protocols for this study were performed according to the guidelines by the Laboratory Animal Center of Hunan Province (Reference number: No. SCXK (Xiang) 2018-0006). All operations were approved by the Animal Experiment Ethics Committee, College of Biology, Hunan University.

Table S1. Comparison of the kinetic parameters of CoOOH@Cu nanosheet and other nanoenzyme or enzyme.

Catalyst	Concentration	Substrate	Km(mM)	Vmax(M/s)	Reference
EMSN-AuNPs	112 μg/mL	H_2O_2	119.2	5.258×10^{-8}	1
C-Dots	50 μg/mL	H_2O_2	26.77	3.061×10^{-7}	2
Au@Pt@SiO2	0.0625 nM	H_2O_2	121.8	6.193×10^{-7}	3
Fe3O4 MNPs	40 μg/mL	H_2O_2	154	9.78×10^{-8}	4
HRP	10 μg/mL	H_2O_2	13.2	5.53×10^{-6}	-
CoOOH@Cu nanosheet	50 μg/mL	H_2O_2	127.3	2.54×10^{-6}	Our work

Km is the Michaelis constant, Vmax is the maximal reaction velocity.

Table S2. Detection of glucose in rat serum sample.

Samples	glucose added (μM)	Glucose Detection					
		Colorimetric	RSD (%)	Recovery (%)	DPV	RSD (%)	Recovery (%)
Diluted rat serum	50	48.73	2.56%	97.46%	50.97	2.56%	101.94%
	100	102.60	2.12%	102.60%	103.77	3.46%	103.77%
	200	192.50	1.96%	96.25%	206.42	4.37%	103.21%
Recovery (%) = $[(c_{Found} - c_{Blank}) / c_{Added}]$ *100%							

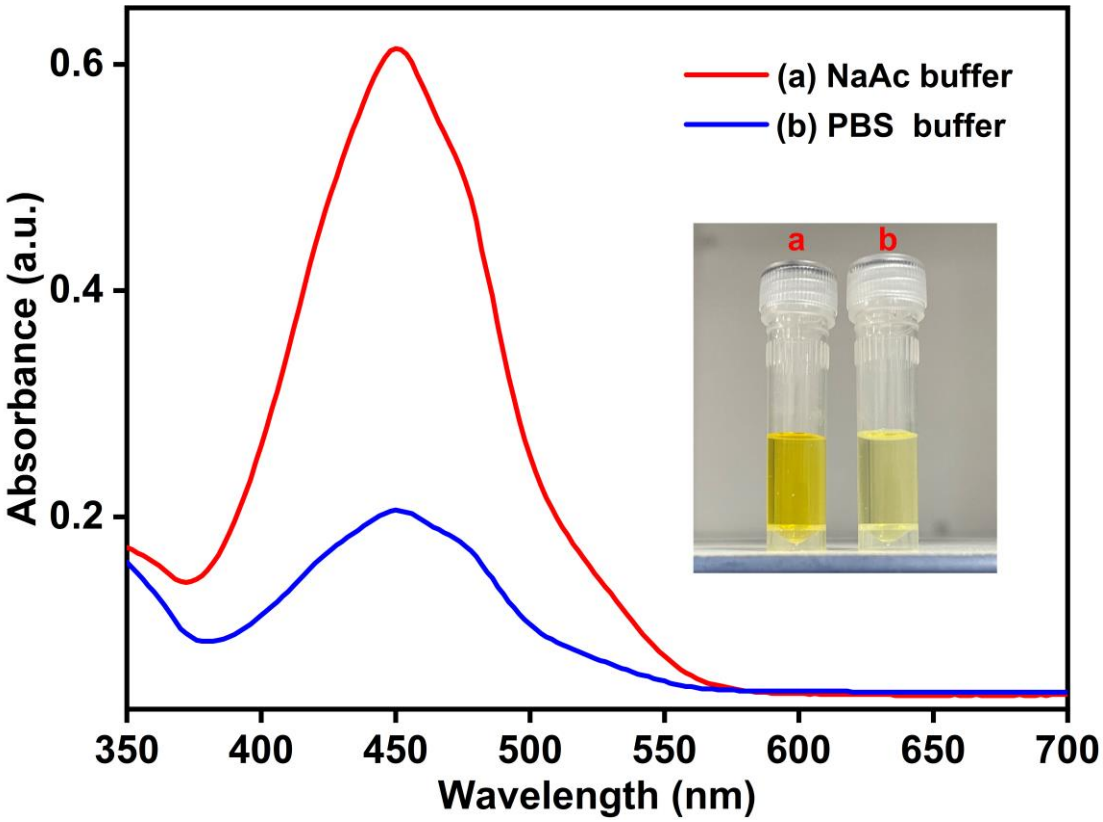

Figure S1. The UV-vis absorption spectrum of CoOOH nanosheet incubation with OPD and H_2O_2 in NaAc and PBS buffer (pH = 4.0), respectively. Insert: visible images of corresponding samples.

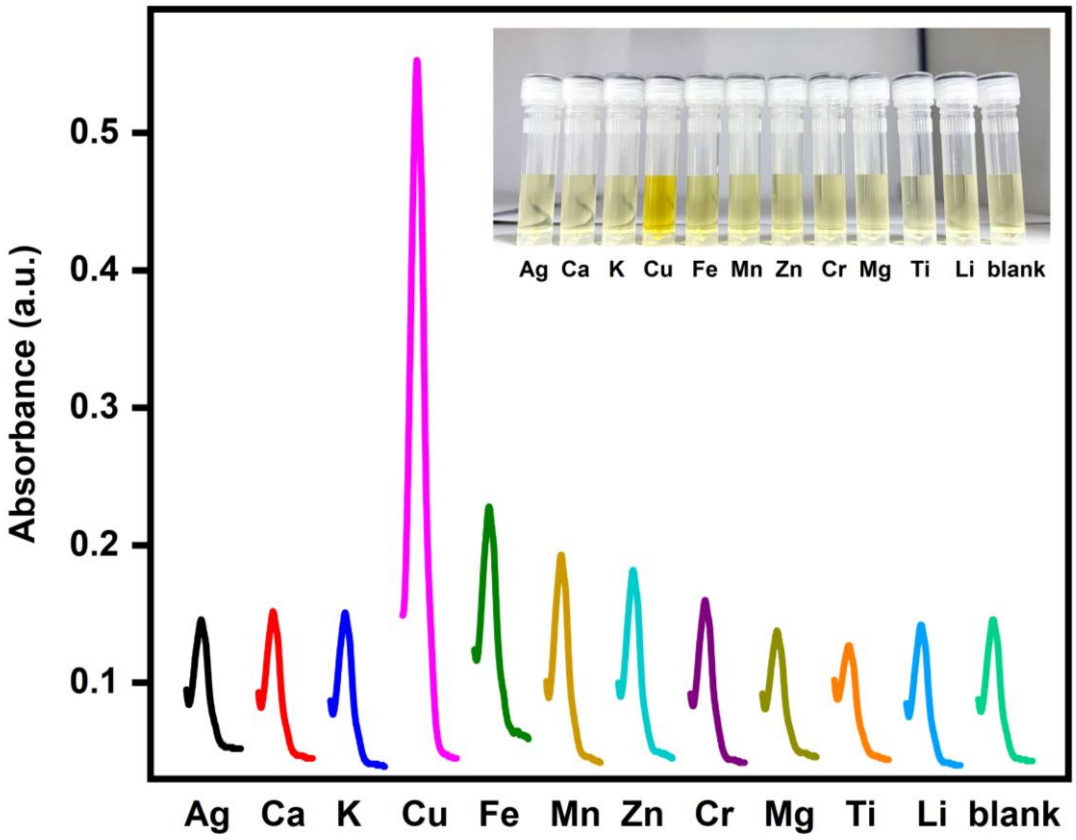

Figure S2. Different metal element coupled CoOOH and its peroxidase-like activity towards OPD and H_2O_2 in PBS buffer (pH = 4.0) including Ag, Ca, K, Cu, Fe, Mn, Zn, Cr, Mg, Ti, Li and blank group, respectively. Insert: visible images of all samples from Ag to blank (Ag : Ag coupled CoOOH, blank : CoOOH).

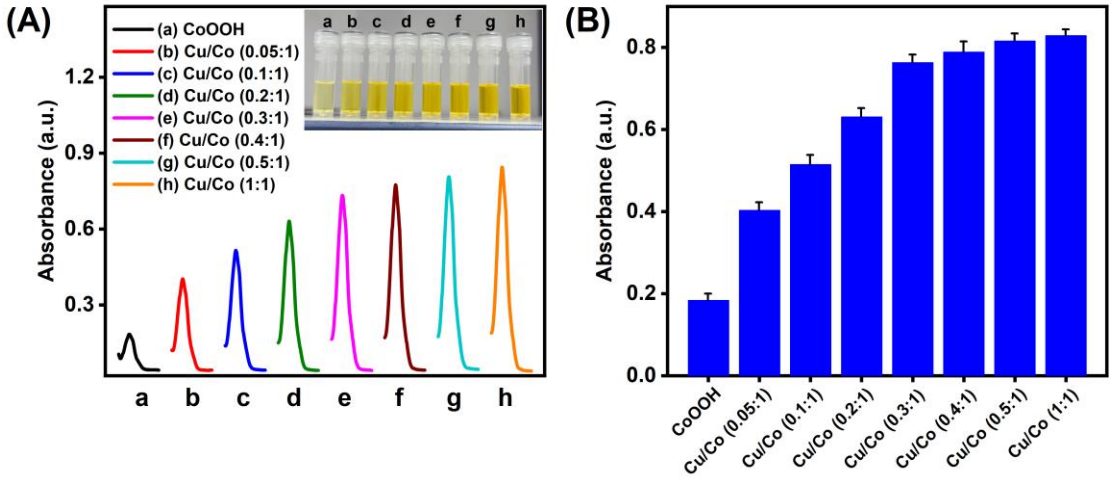

Figure S3. **(A)** The UV-vis absorption spectrum of CoOOH, CoOOH@Cu (Cu:Co = 0.05:1), CoOOH@Cu (Cu:Co = 0.1:1), CoOOH@Cu (Cu:Co = 0.2:1), CoOOH@Cu (Cu:Co = 0.3:1), CoOOH@Cu (Cu:Co = 0.4:1), CoOOH@Cu (Cu:Co = 0.5:1), CoOOH@Cu (Cu:Co = 1:1) incubating with OPD and H_2O_2 in NaAc buffer (pH = 4.0), respectively. Insert: visible images of corresponding samples from a to h; **(B)** The absorbance at 450 nm of CoOOH, CoOOH@Cu (Cu:Co = 0.05:1), CoOOH@Cu (Cu:Co = 0.1:1), CoOOH@Cu (Cu:Co = 0.2:1), CoOOH@Cu (Cu:Co = 0.3:1), CoOOH@Cu (Cu:Co = 0.4:1), CoOOH@Cu (Cu:Co = 0.5:1), CoOOH@Cu (Cu:Co = 1:1) incubating with OPD and H_2O_2 in NaAc buffer (pH = 4.0), respectively. Error bar stands for three independent experiments (n=3).

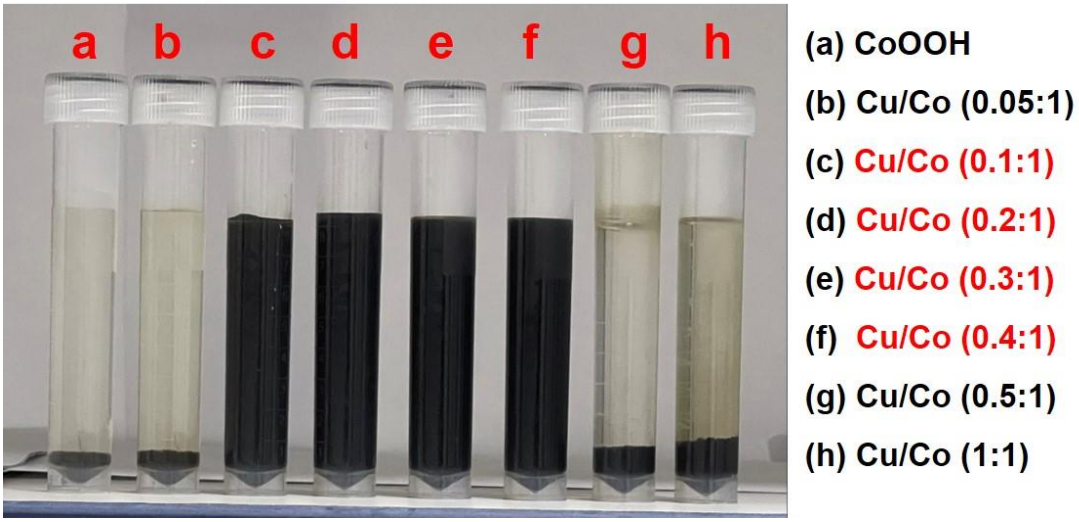

Figure S4. The white light image of (a) CoOOH, (b) CoOOH@Cu (0.05:1), (c) CoOOH@Cu (0.1:1), (d) CoOOH@Cu (0.2:1), (e) CoOOH@Cu (0.3:1), (f) CoOOH@Cu (0.4:1), (g) CoOOH@Cu (0.5:1), (h) CoOOH@Cu (1:1).

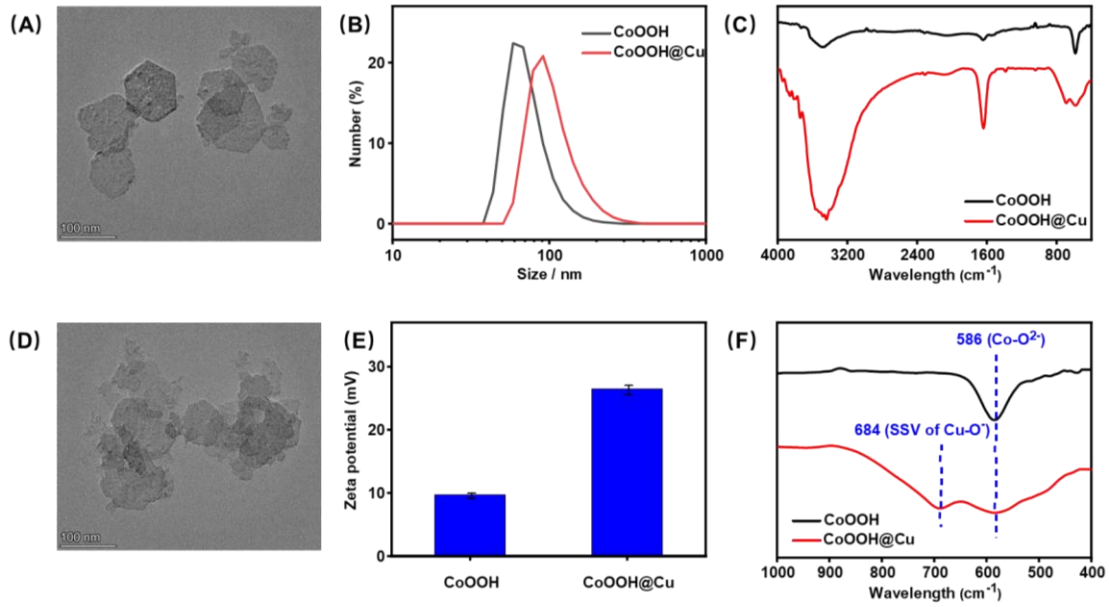

Figure S5. (A) TEM image of the CoOOH nanosheets; (B) size distributions of CoOOH and CoOOH@Cu; (C) full FTIR spectra of CoOOH and CoOOH@Cu; (D) TEM image of CoOOH@Cu; (E) mean zeta potentials of CoOOH and CoOOH@Cu; (F) high-resolution peak fitting FTIR spectra of CoOOH and CoOOH@Cu. Error bar stands for three independent experiments (n = 3).

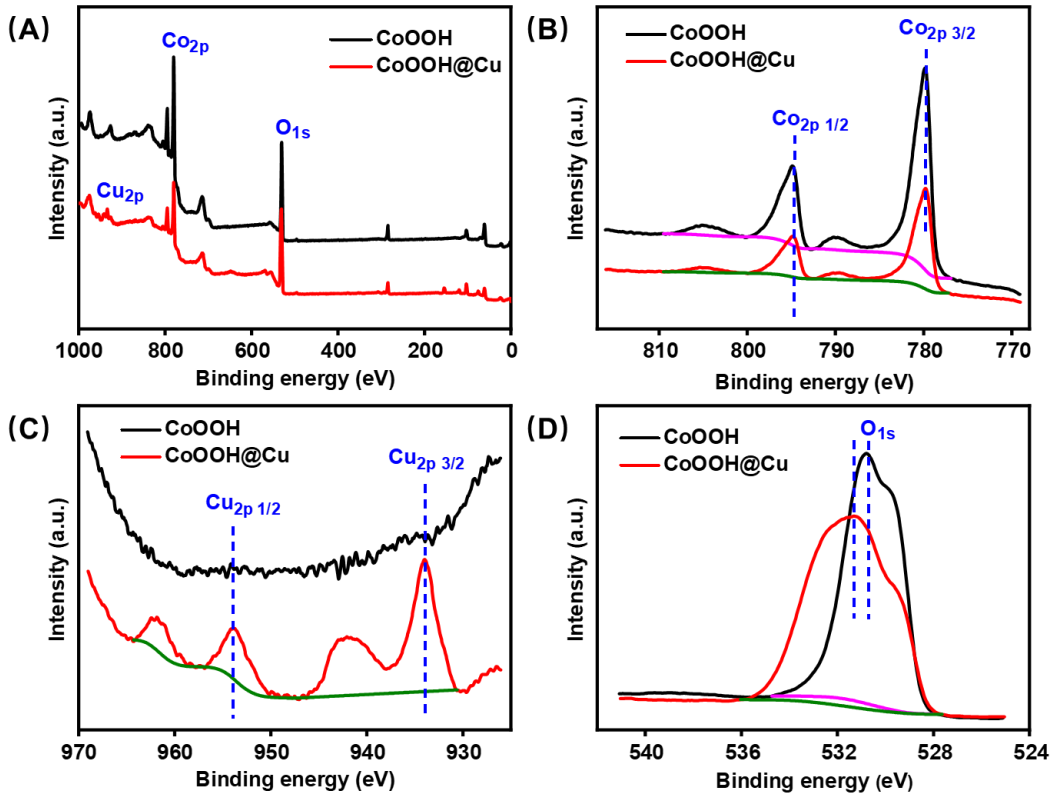

Figure S6. **(A)** The full XPS spectrum of CoOOH and CoOOH@Cu nanosheet; **(B)** The Co 2p XPS spectrum of CoOOH and CoOOH@Cu nanosheet; **(C)** The Cu 2p XPS spectrum of CoOOH and CoOOH@Cu nanosheet; **(D)** The O 1s XPS spectrum of CoOOH and CoOOH@Cu nanosheet.

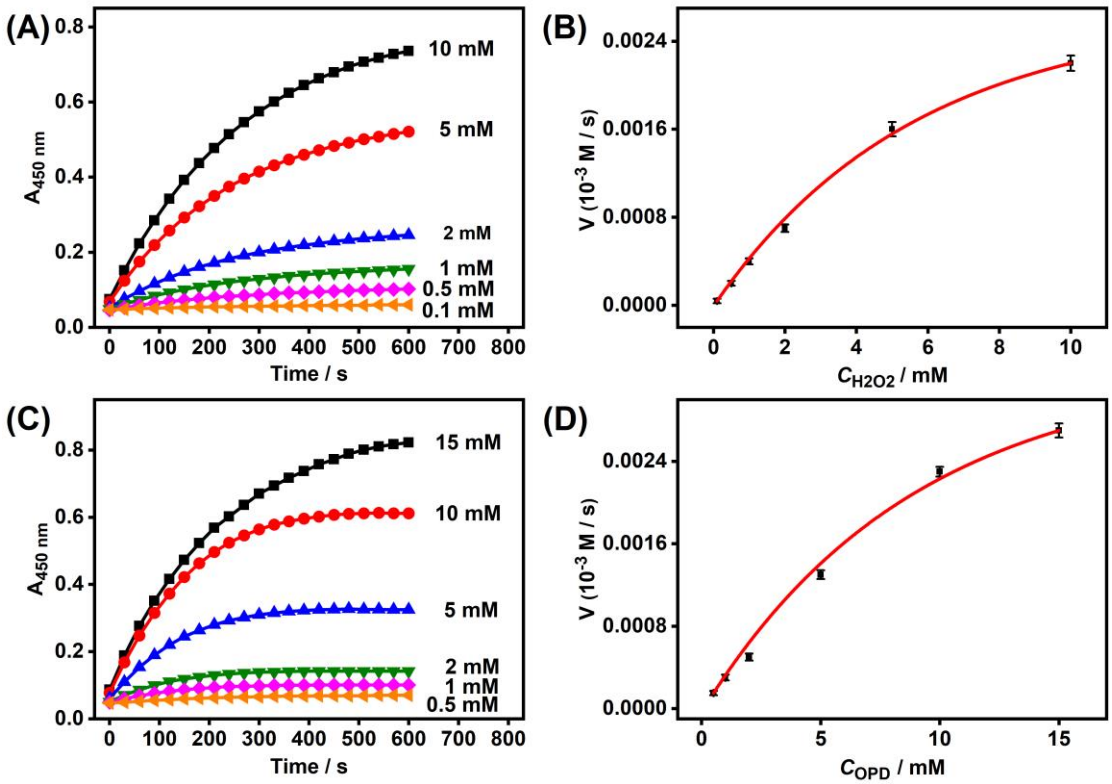

Figure S7. (A) UV dynamic scanning of HRP with 15 mM OPD and various concentration of H_2O_2 from 10, 5, 2, 1, 0.5 to 0.1 mM, respectively; **(B)** Steady-state kinetic assay of HRP with 15 mM OPD and various concentration of H_2O_2 from 10, 5, 2, 1, 0.5 to 0.1 mM, respectively; **(C)** UV dynamic scanning of HRP with 10 mM H_2O_2 and various concentration of OPD from 15, 10, 5, 2, 1, to 0.5 mM, respectively; **(D)** Steady-state kinetic assay of HRP with 10 mM H_2O_2 and various concentration of OPD from 15, 10, 5, 2, 1, to 0.5 mM, respectively. Error bar stands for three independent experiments (n=3).

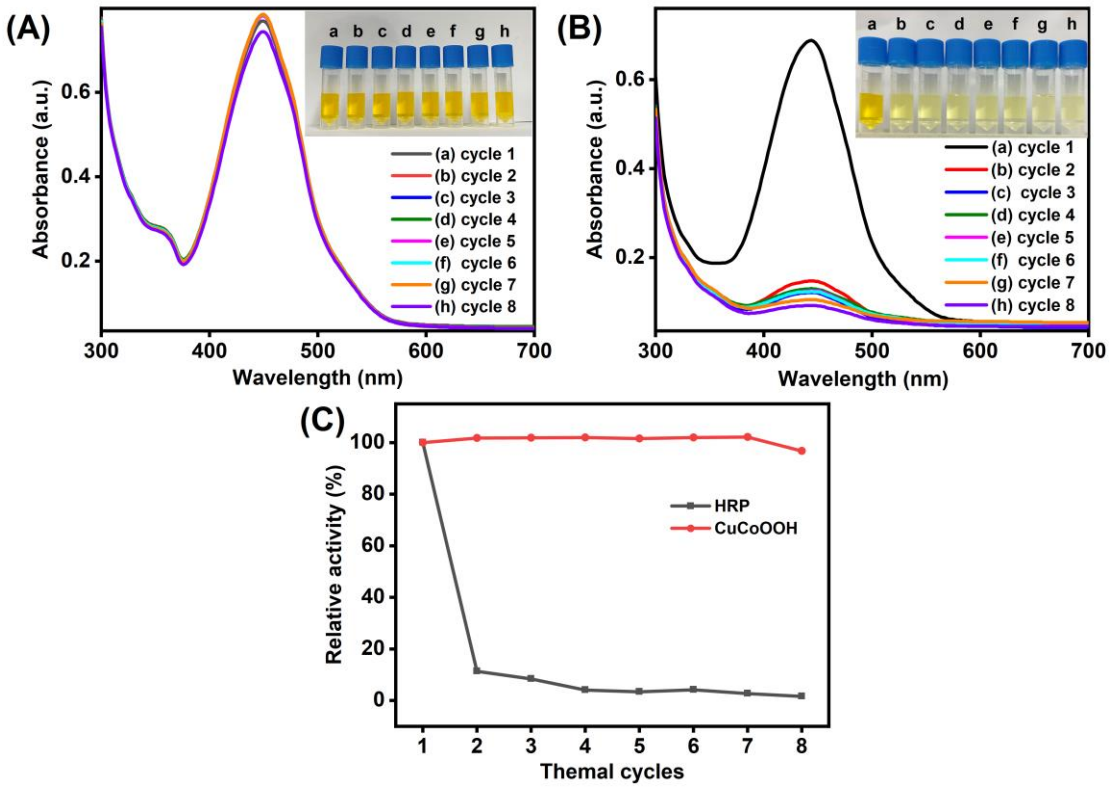

Figure S8. (A) The UV-vis absorption spectrum of CoOOH@Cu incubating with OPD and H_2O_2 in NaAc buffer (pH = 4.0) with different thermal cycles, respectively. Insert: visible images of corresponding samples from a to h; **(B)** The UV-vis absorption spectrum of HRP enzyme incubation with OPD and H_2O_2 in NaAc buffer (pH = 5.0) with different thermal cycles, respectively. Insert: visible images of corresponding samples from a to h; **(C)** The relative activity (100%) of HRP enzyme and CoOOH@Cu nanoenzyme incubating with OPD and H_2O_2 in NaAc buffer with different thermal cycles, respectively.

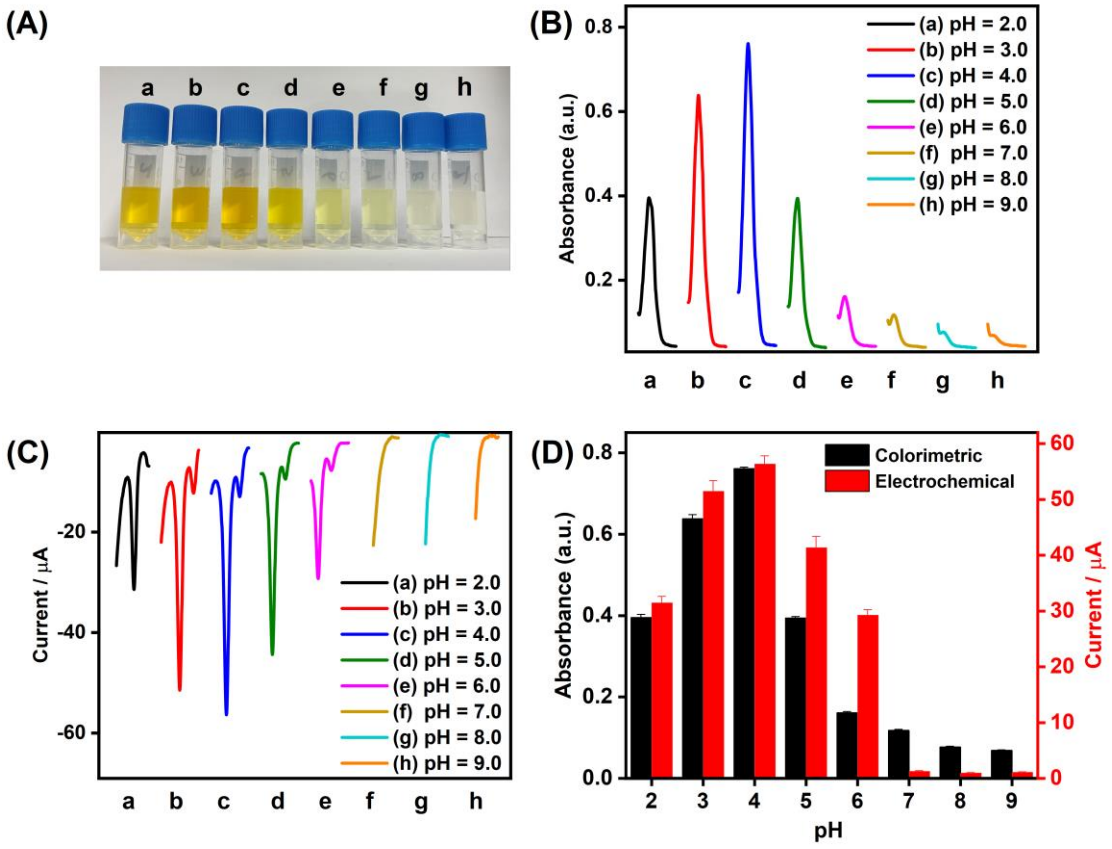

Figure S9. **(A)** Visible images of CoOOH@Cu incubating with OPD and H_2O_2 in NaAc buffer with different pH from 2.0 to 9.0 (corresponding samples from a to h), respectively; **(B)** The UV-vis absorption spectrum of CoOOH@Cu incubating with OPD and H_2O_2 in NaAc buffer with different pH from 2.0 to 9.0, respectively; **(C)** The DPV response of CoOOH@Cu incubating with OPD and H_2O_2 in NaAc buffer with different pH from 2.0 to 9.0, respectively; **(D)** The UV-vis absorbance and DPV response of CoOOH@Cu incubating with OPD and H_2O_2 in NaAc buffer with different pH from 2.0 to 9.0, respectively. Error bar stands for three independent experiments (n=3).

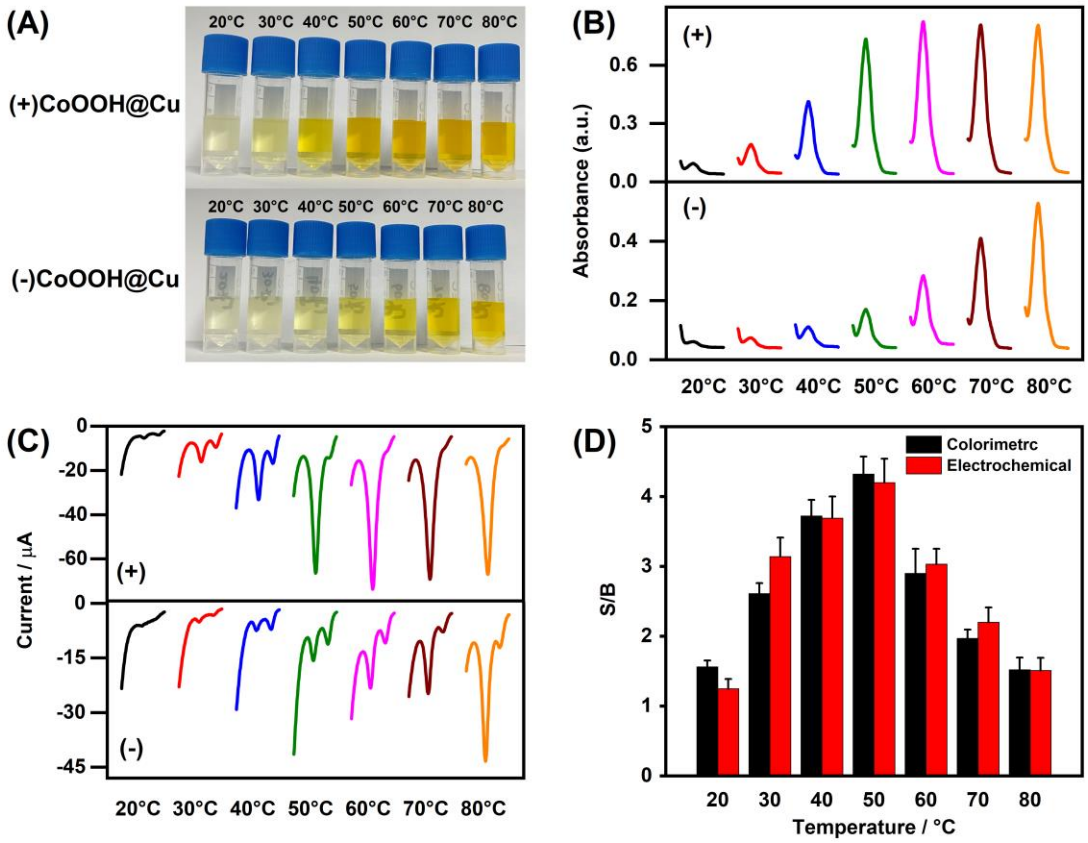

Figure S10. (A) Visible images of OPD incubating with H_2O_2 in the presence of CoOOH@Cu (+) and in the absence of CoOOH@Cu (-) under different temperature from 20 to 80 °C, respectively; **(B)** The UV-vis absorption spectrum of OPD incubating with H_2O_2 in the presence of CoOOH@Cu (+) and in the absence of CoOOH@Cu (-) under different temperature from 20 to 80 °C, respectively; **(C)** The UV-vis absorption spectrum of OPD incubating with H_2O_2 in the presence of CoOOH@Cu (+) and in the absence of CoOOH@Cu (-) under different temperature from 20 to 80 °C, respectively; **(D)** the Signal Background ratio model (S/B) of OPD incubating with H_2O_2 in the presence of CoOOH@Cu (+) and in the absence of CoOOH@Cu (-) under different temperature from 20 to 80 °C, respectively. Error bar stands for three independent experiments (n=3).

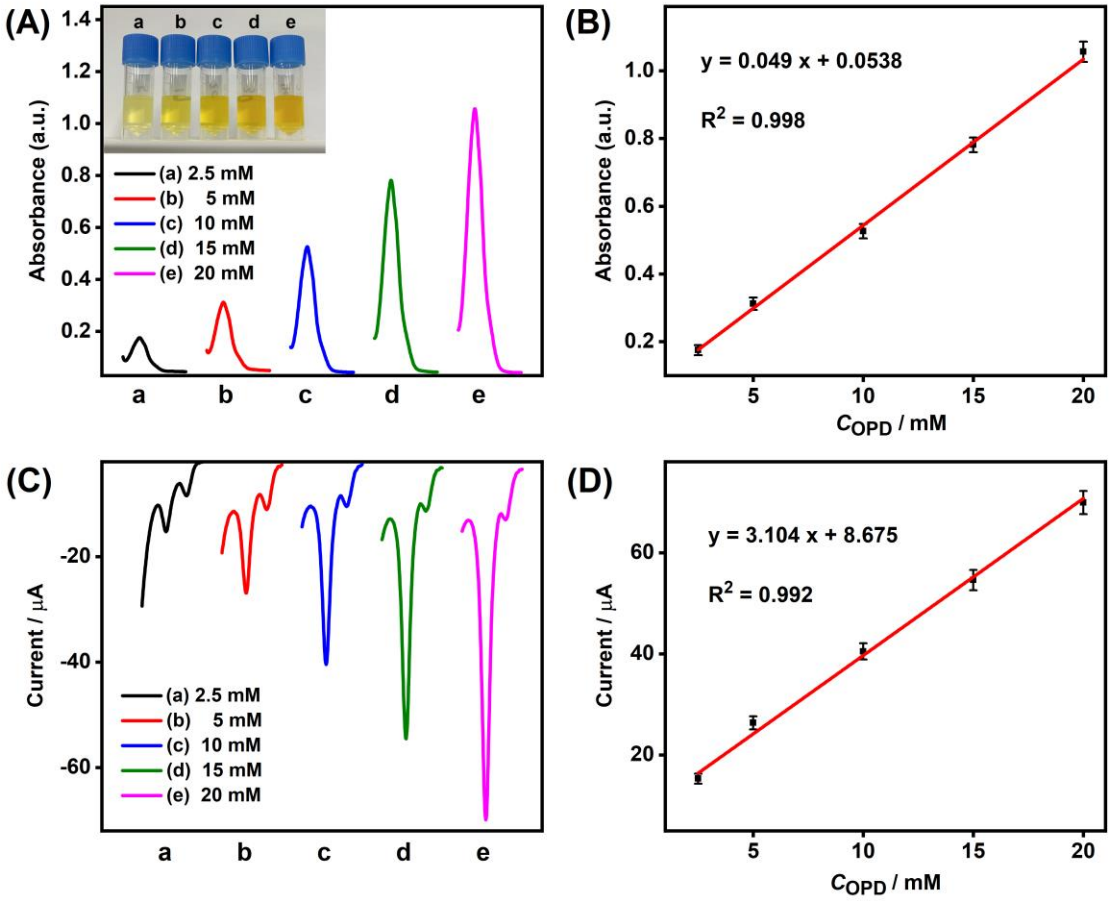

Figure S11. (A) The UV-vis absorption spectrum of CoOOH@Cu incubating with H_2O_2 in NaAc buffer (pH = 4.0) and different concentration of OPD from 2.5 mM to 20 mM, respectively. Insert: visible images of corresponding samples from a to e; **(B)** the linear relationship of UV absorbance at 450 nm and the different concentration of OPD incubating with CoOOH@Cu, H_2O_2 in NaAc buffer from 2.5 mM to 20 mM, respectively; **(C)** the DPV response of CoOOH@Cu incubating with H_2O_2 in NaAc buffer (pH = 4.0) and different concentration of OPD from 2.5 mM to 20 mM, respectively; **(D)** the linear relationship of DPV current and the different concentration of OPD incubating with CoOOH@Cu, H_2O_2 in NaAc buffer from 2.5 mM to 20 mM, respectively. Error bar stands for three independent experiments (n=3).

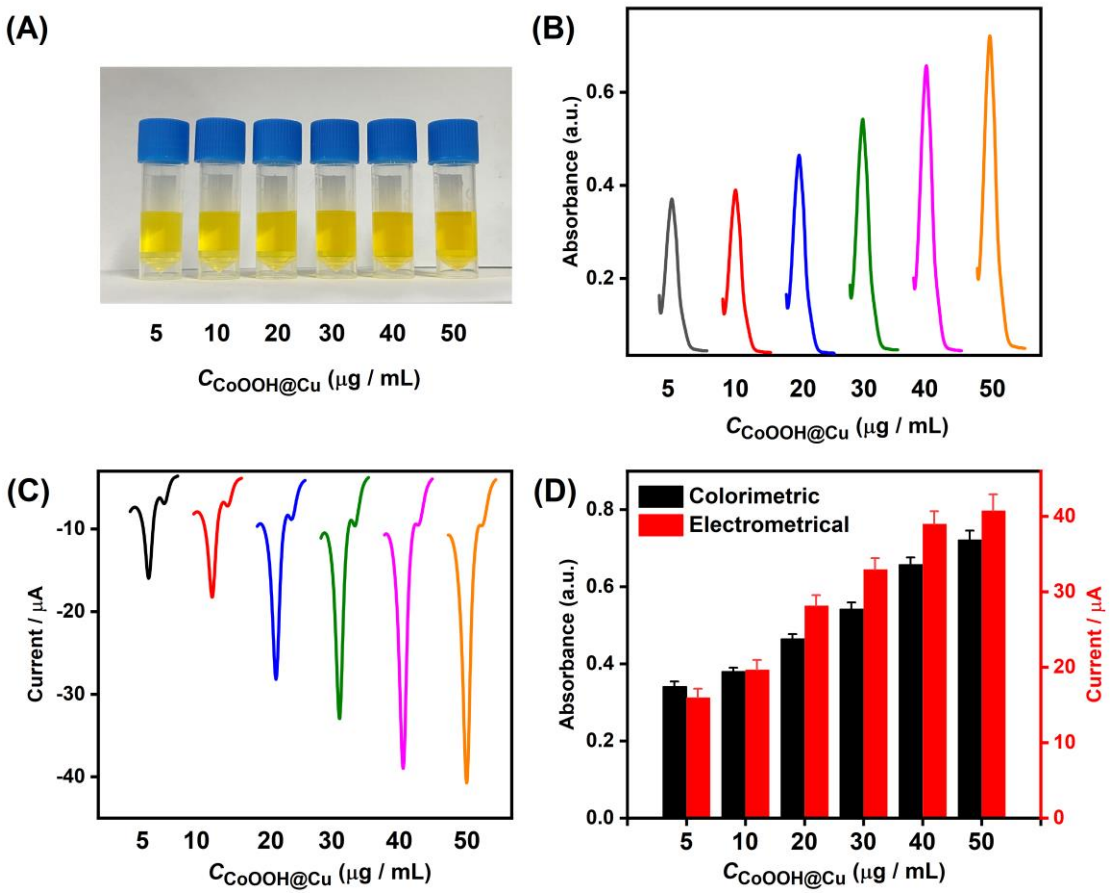

Figure S12. (A) Visible images of OPD and H_2O_2 in NaAc buffer (pH = 4.0) incubating with different concentration of CoOOH@Cu from 5 μg/mL, 10 μg/mL, 20 μg/mL, 30 μg/mL, 40 μg/mL, 50 μg/mL, respectively; **(B)** the UV-vis absorption spectrum of OPD and H_2O_2 in NaAc buffer incubating with different concentration of CoOOH@Cu from 5 μg/mL, 10 μg/mL, 20 μg/mL, 30 μg/mL, 40 μg/mL, 50 μg/mL, respectively; **(C)** the DPV response of OPD and H_2O_2 in NaAc buffer incubating with different concentration of CoOOH@Cu, respectively; **(D)** the UV-vis absorbance and DPV response of OPD and H_2O_2 in NaAc buffer incubating with different concentration of CoOOH@Cu, respectively. Error bar stands for three independent experiments (n=3).

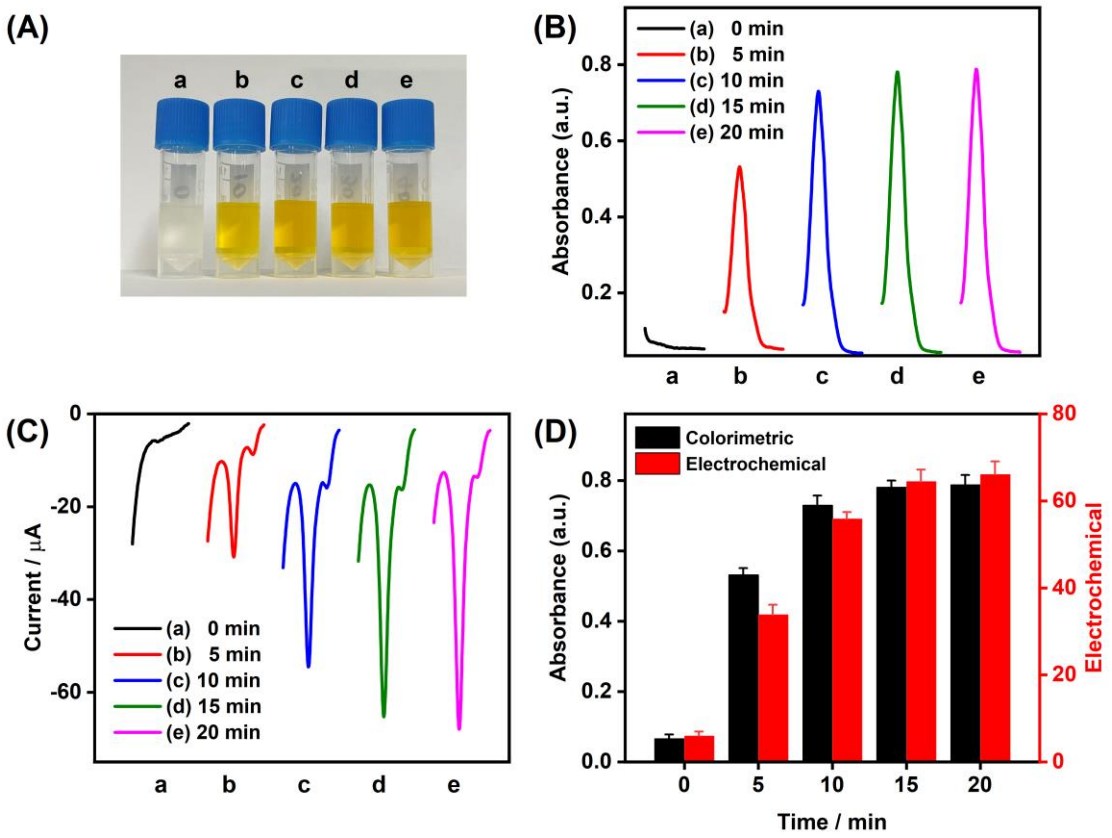

Figure S13. (A) Visible images of CoOOH@Cu incubating with OPD and H_2O_2 in NaAc buffer (pH = 4.0) for different time from 0 min to 20 min, respectively (corresponding samples from a to e); **(B)** The UV-vis absorption spectrum of CoOOH@Cu incubating with OPD and H_2O_2 in NaAc buffer for different time from 0 min to 20 min, respectively; **(C)** The DPV response of CoOOH@Cu incubating with OPD and H_2O_2 in NaAc buffer for different time from 0 min to 20 min, respectively; **(D)** The UV-vis absorbance and DPV response of CoOOH@Cu incubating with OPD and H_2O_2 in NaAc buffer for different time from 0 min to 20 min, respectively. Error bar stands for three independent experiments (n=3).

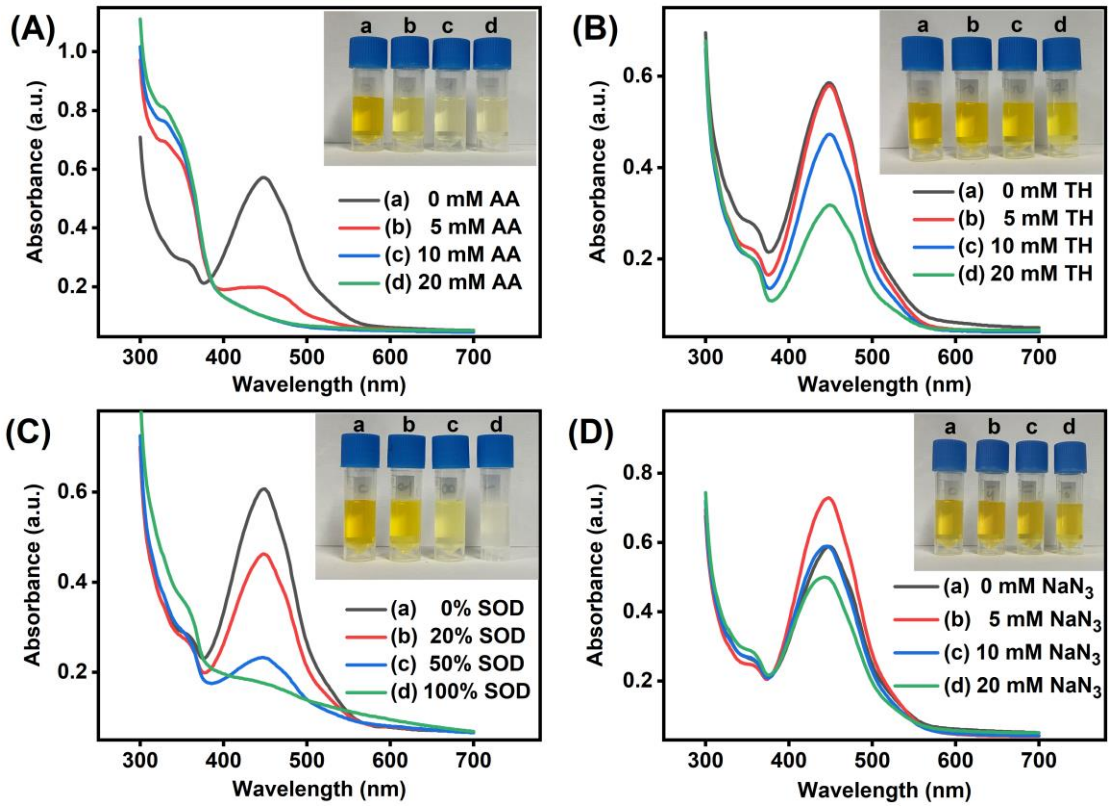

Figure S14. (A) The UV-vis absorption spectrum of CoOOH@Cu incubating with OPD and H_2O_2 in NaAc buffer (pH = 4.0) with different concentration of radical scavenger AA from 0, 5 mM, 10 mM and 20 mM, respectively (corresponding samples from a to d); **(B)** the UV-vis absorption spectrum of CoOOH@Cu incubating with OPD and H_2O_2 in NaAc buffer with different concentration of radical scavenger TH from 0, 5 mM, 10 mM and 20 mM, respectively (corresponding samples from a to d); **(C)** the UV-vis absorption spectrum of CoOOH@Cu incubating with OPD and H_2O_2 in NaAc buffer with different concentration of radical scavenger SOD from 0, 20 %, 50 % and 100 %, respectively (corresponding samples from a to d) ; **(D)** the UV-vis absorption spectrum of CoOOH@Cu incubating with OPD and H_2O_2 in NaAc buffer with different concentration of radical scavenger NaN_3 from 0, 5 mM, 10 mM and 20 mM, respectively (corresponding samples from a to d).

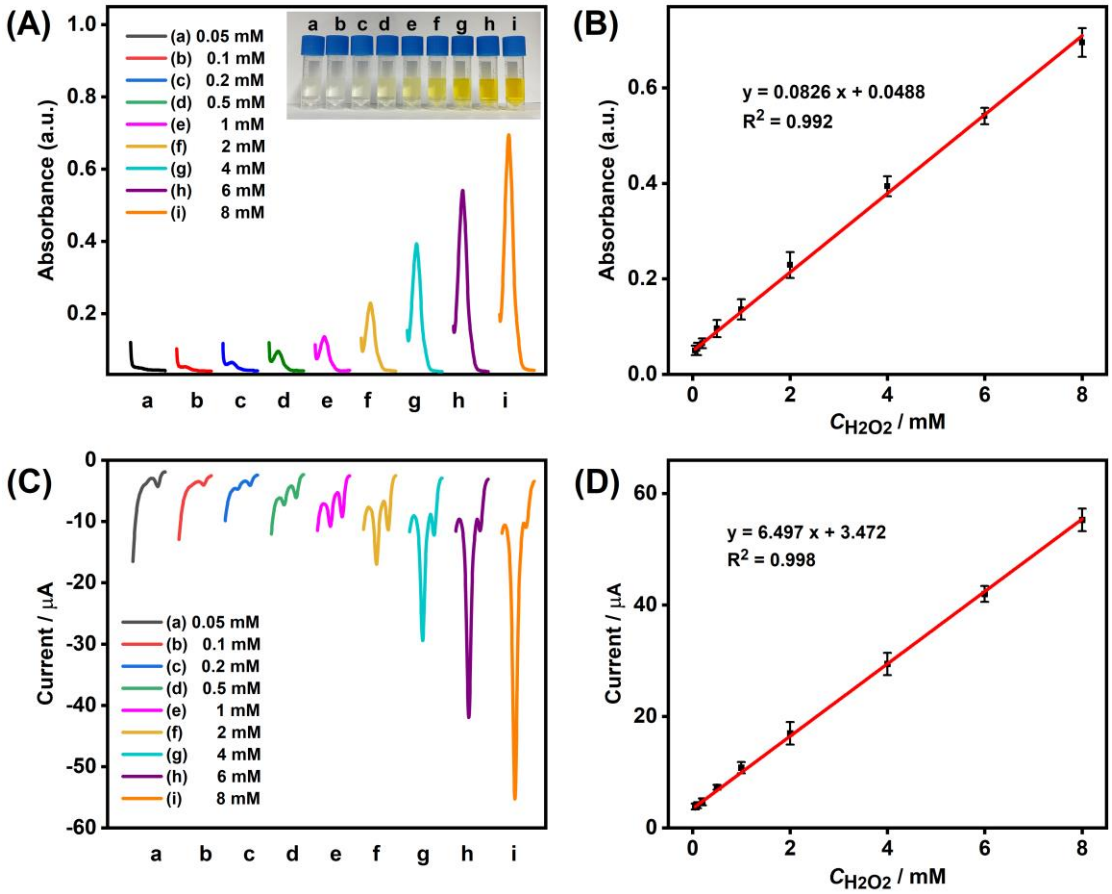

Figure S15. (A) The UV-vis absorption spectrum of this biosensing system upon the addition of H_2O_2 with different concentrations from 50 μM to 8 mM, respectively. Insert: the photograph of corresponding samples; **(B)** the linear relationship between the UV absorbance at 450 nm and H_2O_2 concentration; **(C)** the DPV current of this biosensing system upon the addition of H_2O_2 with different concentrations from 50 μM to 8 mM, respectively; **(D)** the linear relationship between DPV current and H_2O_2 concentration. Error bar stands for three independent experiments (n=3).

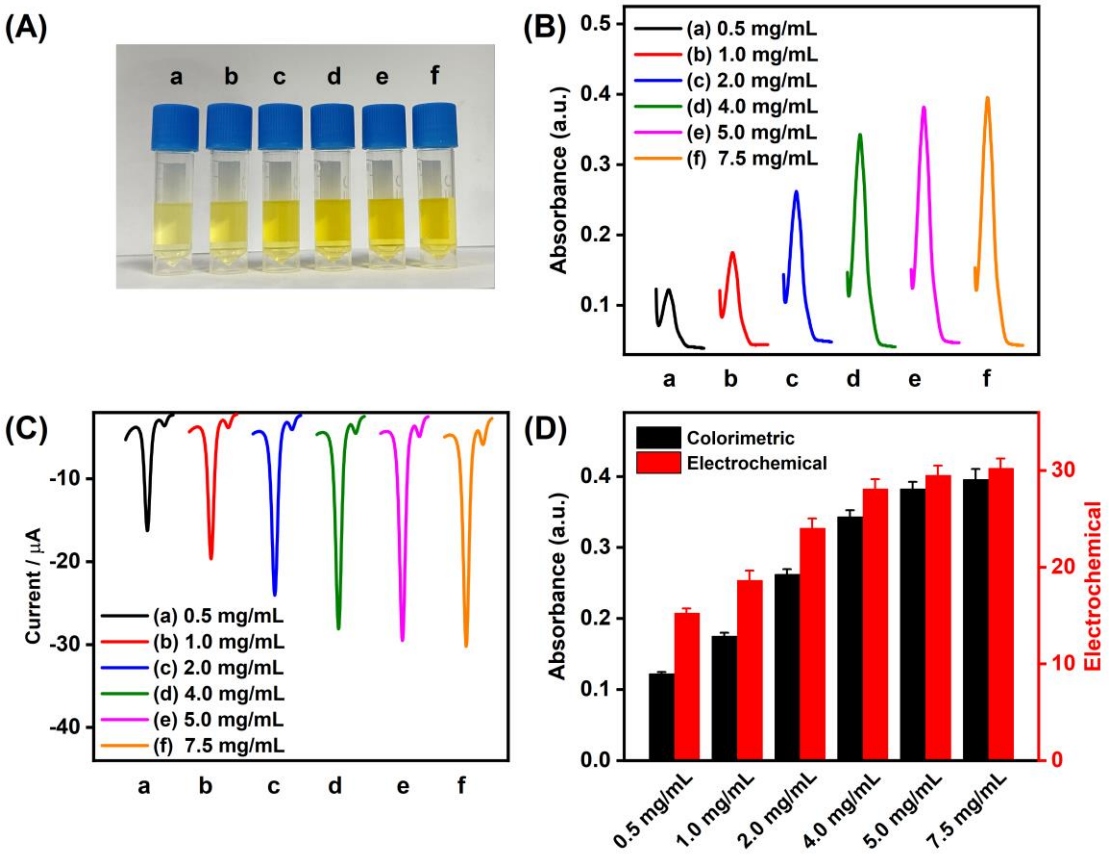

Figure S16. (A) Visible images of OPD, H_2O_2 and glucose in NaAc buffer (pH = 4.0) incubating with different concentration of Glucose Oxidase (GOx) from 0.5 mg/mL to 7.5 mg/mL, respectively (visible images of corresponding samples from a to f); **(B)** The UV-vis absorption spectrum of OPD, H_2O_2 and glucose in NaAc buffer incubating with different concentration of GOx from 0.5 mg/mL to 7.5 mg/mL, respectively; **(C)** The DPV response of OPD, H_2O_2 and glucose in NaAc buffer incubating with different concentration of GOx from 0.5 mg/mL to 7.5 mg/mL, respectively; **(D)** The UV-vis absorbance and DPV response of OPD, H_2O_2 and glucose in NaAc buffer incubating with different concentration of GOx from 0.5 mg/mL to 7.5 mg/mL, respectively. Error bar stands for three independent experiments (n=3).

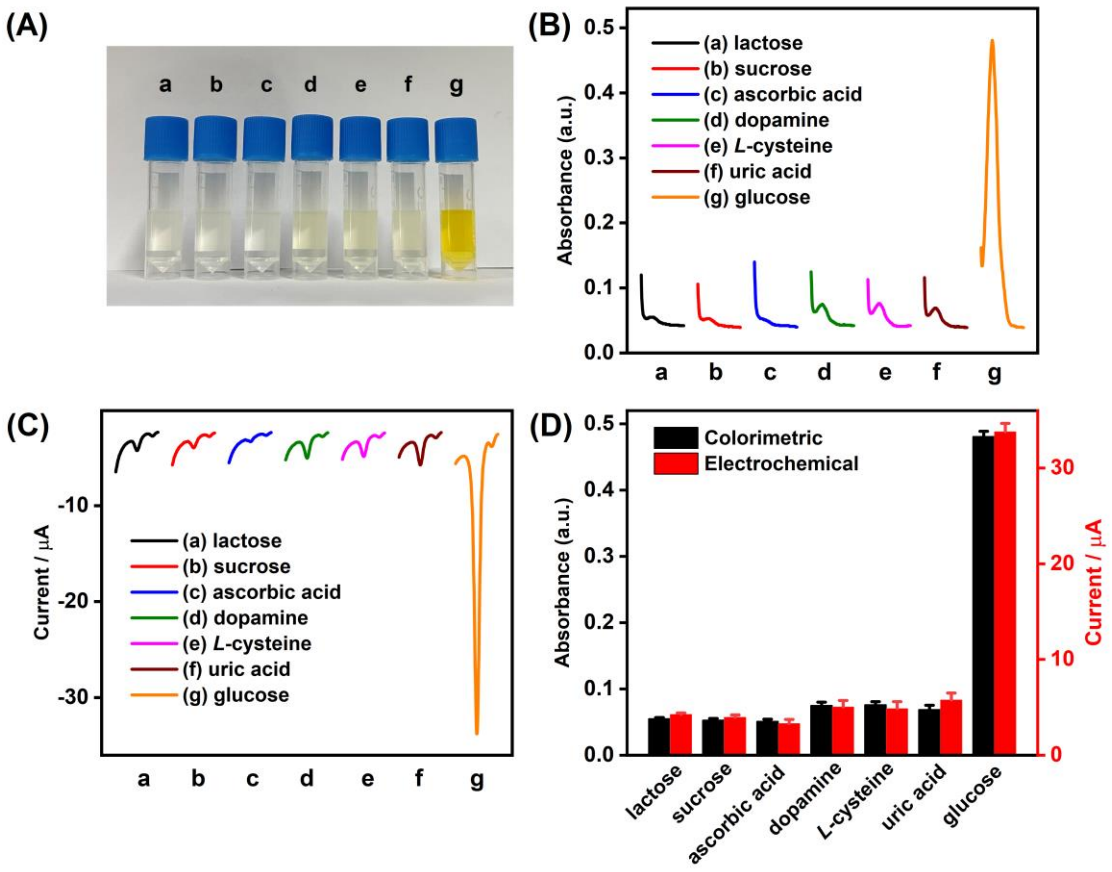

Figure S17. (A) Visible images of OPD, H_2O_2 and GOx in NaAc buffer (pH = 4.0) incubating with different interferences including lactose (25 mM), sucrose (25 mM), ascorbic acid (25 mM), dopamine (25 mM), *L*-cysteine (25 mM), uric acid (25 mM) and glucose (2.5 mM), respectively (corresponding samples from a to g); **(B)** The UV-vis absorption spectrum of OPD, H_2O_2 and GOx in NaAc buffer incubating with different interferences including lactose, sucrose, ascorbic acid, dopamine, L-cysteine, uric acid and glucose, respectively; **(C)** The DPV response of OPD, H_2O_2 and GOx in NaAc buffer incubating with different interferences including lactose, sucrose, ascorbic acid, dopamine, *L*-cysteine, uric acid and glucose, respectively; **(D)** The UV-vis absorbance and DPV response of OPD, H_2O_2 and GOx in NaAc buffer incubating with different interferences including lactose, sucrose, ascorbic acid, dopamine, *L*-cysteine, uric acid and glucose, respectively. Error bar stands for three independent experiments (n=3).

Reference

(1) Lin, Y. H.; Li, Z. H.; Chen, Z. W.; Ren, J. S.; Qu, X. G. Mesoporous Silica-Encapsulated Gold Nanoparticles as Artificial Enzymes for Self-Activated Cascade Catalysis. *Biomaterials* **2013**, 34, 2600-2610.

(2) Shi, W. B.; Wang, Q. L.; Long, Y. J.; Cheng, Z. L.; Chen, S. H.; Zheng, H. Z.; Huang, Y. M. Carbon Nanodots as Peroxidase Mimetics and Their Applications to Glucose Detection. *Chem. Commun.*, **2011**, 47, 6695-6697.

(3) Li, A. Y.; Long, L.; Liu, F. S.; Liu, J. B.; Wu, X. C.; Ji, Y. L. Antigen-Labeled Mesoporous Silica-Coated Au-Core Pt-Shell Nanostructure: A Novel Nanoprobe for Highly Efficient Virus Diagnosis. *J. Biol. Eng.* **2019**, 13:87.

(4) Gao, L. Z.; Zhuang, J.; Nie, L.; Zhang, J. B.; Zhang, Y.; Gu, N.; Wang, T. H.; Feng, J.; YANG, D. L.; Perrett, S.; Yan, X. Y. Intrinsic Peroxidase-Like Activity of Ferromagnetic Nanoparticles. *Nat. Nanotechnol.* **2007**, 2, 577-583.